Vol. 35, No. 3 (2013) 217-224

Tribology in Industry

www.tribology.fink.rs

RESEARCH

Topographic and Electrochemical Ti6Al4V Alloy Surface Characterization in Dry and Wet Reciprocating Sliding

Z. Doni [a], M. Buciumeanu [a], Liviu Palaghian [a]

[a] *"Dunarea de Jos" University of Galati, Romania.*

Keywords:

Reciprocating Wear
Light Alloy
Roughness
Surface Integrity

Corresponding author:

Zinaida Doni
"Dunarea de Jos" University of Galati, Romania.
E-mail: zinaida.doni@yahoo.com

A B S T R A C T

This present paper shows the behavior of functional integrity state of a Ti6Al4V alloy under reciprocating wear sliding conditions in a comparative way for two different counter *materials, steel and ceramic balls in dry and corrosive environment (3.5 % NaCl). The surface integrity analysis of the dry reciprocating wear tests was based on the evolution of the roughness parameters with the applied load. In the case of reciprocating wear tests in corrosive environment the surface integrity analysis was based on electrochemical parameters. Comparative analysis of the evolution of the roughness parameters with the applied load shows a higher stability of the Ti6Al4V/Al_2O_3 contact pair, while from the point of view of the electrochemical parameters the tribological properties are worse than Ti6Al4V/steel ball contact pair.*

1. INTRODUCTION

The required functional properties of the contact surfaces under relative motion are closely related to the surface integrity state. The modifications of the superficial layer during the machining process and subsequently during service life have an important role in defining the surface integrity state. Thus Griffiths [1] proposed to define the surface integrity state based the mechanical, chemical, metallurgical and topographical characteristics of the superficial layer and their relation to the functional performance.

Bellows and Tishler [2] stated that there are five types of modifications of the superficial layer during the machining process of a surface: mechanical, metallurgical, chemical, thermal and electrical. These characteristics are changing during the service life. Besides other functional characteristics, such as fatigue resistance, correlation between surface roughness parameters (R_a, R_z, R_k, etc.), and the wear rate has an important role during the friction processes of the contact surfaces under relative motion [3-5].

Thus the surface integrity state can be defined not only due to the machining processes of the surface, but also due to the operating processes. This can be called functional integrity state. Generally, it is intended that during the service life to maintain the

same characteristics obtained from the machining process or to have acceptable modifications.

The Ti6Al4V alloy is the most common titanium alloy due to its physical, chemical and mechanical properties, such as: high strength, low density, excellent machinability and excellent corrosive resistance. Some of the most widespread applications of these alloys include aircraft turbine engines, structural components and joints in aeronautics, structural elements in automotive and maritime constructions, medical devices (dental and orthopedic implants) [6,7].

The spontaneously formation of a continue and strong adherent oxide layer in air and also water (e. g. the marine environment, body fluids) provides extensive use of these alloys.

Conventional ceramics materials such as alumina (Al_2O_3) have excellent properties, such as: high hardness and good wear resistance, excellent dielectric properties, high resistance to chemical attack in presence of acids and alkali, high thermal conductivity, high resistance and stiffness, excellent formability and high purity. Due to these properties alumina is widely used in technical applications (e. g. automotive industry and in medical implants).

The general properties of the two types of materials (Ti6Al4V and Al_2O_3) have leaded to the use of these in applications where both wear and corrosion resistant qualities are critical. In these applications, especially under relative motion and under the action of external loads and in active chemical environments, it is mandatory to maintain the surface integrity state during the service life.

In the present paper is presented the evolution of the functional integrity state in a comparative way for two contact pairs (Ti6Al4V/Al_2O_3 and Ti6Al4V/steel ball) in dry and corrosive environment.

2. DRY WEAR AND TRIBOCORROSION FORMULATION

The analysis of the functional integrity state under dry wear conditions is based on the well known Archard's wear law [8]. It says that the amount of the material loss depends on the properties of the contact surfaces, topographical characteristics of the surfaces and test conditions. The most common form of Archard's equation is:

$$\frac{V}{S} = K\frac{F_n}{H} \tag{1}$$

where V - the volumetric material loss of the body, K- the wear coefficient (it is dimensionless and always less than unity), H - the hardness of the softer body in contact, F_n - the applied normal load and S - the sliding distance.

It has been analyzed the amount of material that was removed (wear loss) in the wear process. The surface analysis of the wear tests was based on the evolution of the depth of the wear track (based on the material loss) with the applied load. Another parameter that was analyzed is the final topography of the wear track by using the 3D roughness parameters (S_a – Average Roughness, S_y - Peak-Peak Height, S_q - Root Mean Square Height, S_p - Maximum Peak Height, S_v - Maximum Pit Height).

In the case of reciprocating wear tests in corrosive environment occur the degradation process of surfaces by tribocorrosion. This process includes the interaction between mechanical, chemical and electromechanical processes of wear that lead to loss of weight by adding all these effects [9]:

Wear=mechanical wear process+electrochemical (and/or chemical response) (2)

This process includes the interaction of corrosion with: solid corrosive particles (debris), particles resulted due to abrasive processes, fretting processes, processes under biological solution conditions, and triboxidation related to the mutual interaction process under relative motion conditions of the surfaces.

Generally, oxide layers are formed after the corrosive attack which protects the material from further corrosive attack. But these oxide films are susceptible to the tribological processes that will accelerate the corrosion in these areas. The galvanic activity that results between the worn and unworn surfaces under electrochemical conditions [10], leads to an anodic current I_a, [11]:

$$I_a = k_b \cdot l \cdot f \cdot \left(\frac{F_n}{H}\right)^{1/2} \cdot \int_0^{1/f} i \cdot d\tau \tag{3}$$

where: k_b – proportionality factor; l – sliding length; f – frequency of the reciprocating motion; F_n – normal load; H – surface hardness; i – corrosion current density; τ – time.
Equation (3) can be written as [9]:

$$I_p = k_b \cdot V_s \cdot \left(\frac{F_n}{H}\right)^{1/2} \cdot Q_p \qquad (4)$$

where: V_s – sliding speed; Q_p - passivation charge density [8].

$$Q_p = \int_0 i_{corr} \cdot d\tau \qquad (5)$$

On the other hand, electrochemical wear can be determined based on passivation current

$$V = \frac{I_p \cdot t \cdot M_{mol}}{n \cdot \rho \cdot F} \qquad (6)$$

where: t – time; M – molecular weight; ρ – density; n – valence; I – Faraday's constant.

The corrosion rate [13,14,15] can be determined based on linear polarization and on the Stern-Geary's equation [16] as follows:

$$i_{corr} = \frac{\beta_a \cdot \beta_c}{2.3(\beta_a + \beta_c)} \cdot \frac{1}{R_p} \qquad (7)$$

where: β_a şi β_c cathodic and anodic Tafel slopes (Fig. 1); R_r – polarization resistance.

Thus the tribocorrosion processes can be analysed based on the evolution of the electrochemical parameters β_a, β_c, I_{corr}, E_{corr}.

If in the dry wear conditions the amount of the material loss is determined based on the ration F_n/H, in the case of wear tests in the corrosion environment conditions the wear process is influenced by the electrochemical parameters.

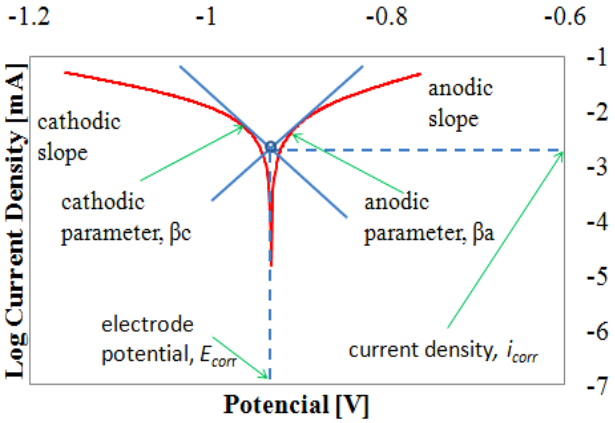

Fig. 1. Typical plot derived by the Tafel extrapolation method.

3. EXPERIMENTAL PROCEDURE

a. Materials

The material contact pairs comparatively studied in this work are: Ti6Al4V/Al_2O_3 and Ti6Al4V/steel ball.

The mechanical properties of the materials used in this study are presented in Table 1 and their chemical composition is given in Tables 2 and 3.

Table 1. Mechanical properties of Ti6Al4V alloy.

Material	Mechanical properties				
	E (GPa)	$\sigma_{0.2}$ (MPa)	σ_r (MPa)	ε_r (%)	HV
Ti6Al4V	115	989	1055	16,1	360
Al2O3 (96%)	300	-	2200		1100
100Cr6	210	1034	1158	15	750

Table 2. Chemical composition (weight %) of Ti6Al4V alloy.

Elements	Al	V	Fe	Sn	Ni
Ti6Al4V	6.1	4.21	0.2	0.003	0,01

Table 3. Chemical composition (weight %) of 100Cr6.

Elements	C	Si	Mn	P	S	Cr	Mo
100Cr6	0.93	0,15	0.25	0.026	0.15	1.35	0.10

b. Experimental test set-up

Reciprocating dry wear tests were carried out on a tribometer type CETR PRO 5003D. The experiments were carried out at a frequency of 1 Hz and the total stroke length of 3 mm during 3 h, using a reciprocating ball-on-plate configuration. Bearing steel and Al_2O_3 balls of 8 mm diameter were used as counterpart. The experiments were carried out at three normal loads 100, 120 and 140 N. Figure 2 presents the schematic test configuration.

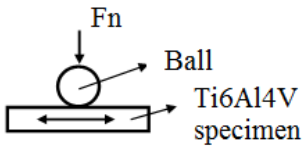

Fig. 2. Schematic specimen-pad contact test configuration (F_n - normal load).

The surface roughness parameters were determined using a 3D profilometer type CETR PRO500. The roughness parameters were obtained by scanning a surface of 500x500 μm, in 200 point on each line. Multiple measurements in different areas on the wear track were carried out to obtain stable roughness values that can be

representative for entire wear track. The 3D images were analyzed by using a processing image soft - Scanning Probe Imagine Processor (SPIP). The 3D roughness parameters used to describe the surface features are S_a – Average Surface Roughness, S_y - Peak-Peak Height, S_q - Root Mean Square Height, S_p - Maximum Peak Height, S_v - Maximum Pit Height. The initial surface roughness parameters studied were S_a =0.14 μm; S_y =3.96 μm; S_q =0.18 μm; S_p =3.34 μm; S_v =0.63 μm.

In corrosive conditions the reciprocating wear tests were carried out under the same conditions, with the contact pairs immersed in the electrolyte - an aqueous solution of 3.5 % NaCl (Fig. 3). The electrochemical characteristics were obtained with a potentiostatic assembly.

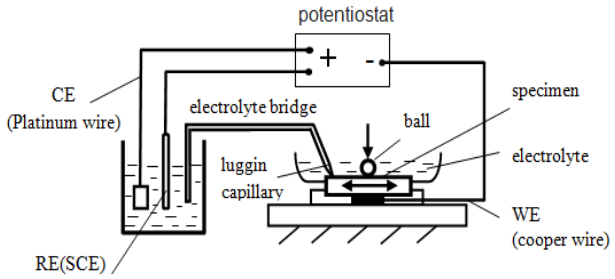

Fig. 3. Schematic of the corrosion wear method.

4. EXPERIMENTAL RESULTS AND DISCUSSIONS

Figure 4 shows the profiles of the wear track at the end of the test for Ti6Al4V/steel ball contact pair for the three normal loads used in this study.

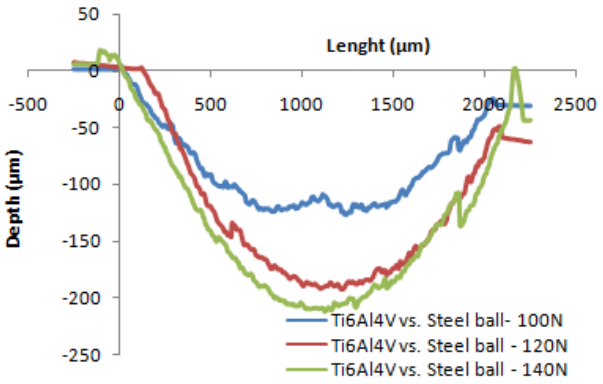

Fig. 4. Evolution of the profiles with the applied normal load.

Figure 5 shows the evolution of the weight loss with increasing applied normal load for both contact pairs.

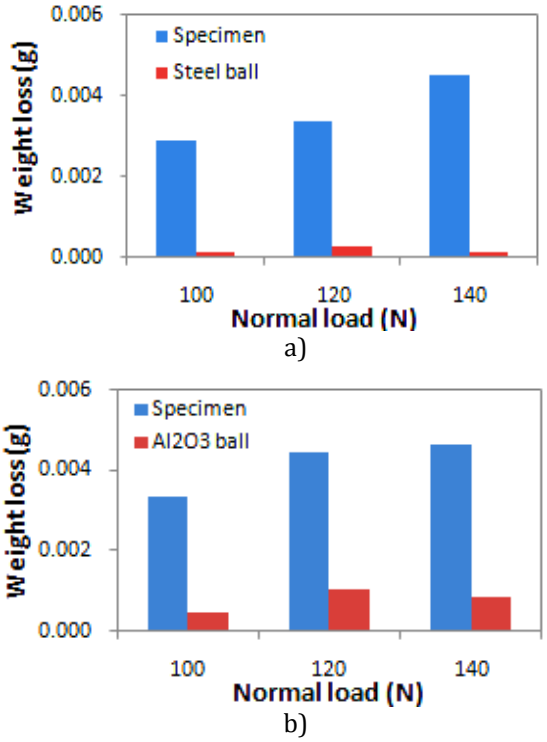

Fig. 5. Evolution of the weight loss with increasing applied normal load: a Ti6Al4V/Al2O3 and b. Ti6Al4V/steel ball.

Regarding the functional integrity in terms of variation with the applied load it is remarked the equivalent level of the weight loss of the steel ball at higher loads (120-140 N) (Figs. 4 and 5).

On the other hand, in the case of Ti6Al4V/Al_2O_3 contact pair can be observed that the weight loss of the alumina ball increases with increasing applied normal load (Fig. 5b).

In the case of Ti6Al4V/Al_2O_3 contact pair can be observed a constant variation of the weight loss of the alumina ball counterpart (Fig. 5a) while in the case of Ti6Al4V/steel ball to the steel ball counterpart (Fig. 5b). Also, the weight loss was higher is the case of the steel ball counterpart compared to the alumina ball counterpart.

The evolution of the roughness parameters with increasing applied normal load over the functional integrity (Fig. 6) shows that in the case of Ti6Al4V/steel ball contact pairs the roughness parameter, S_v, was slightly influenced by the modification of the applied normal load.

In the case of Ti6Al4V/Al_2O_3 contact pair the roughness parameters that changed with increasing applied normal load are S_a (Fig. 6a), S_q (Fig. 6b) and S_y (Fig. 6c).

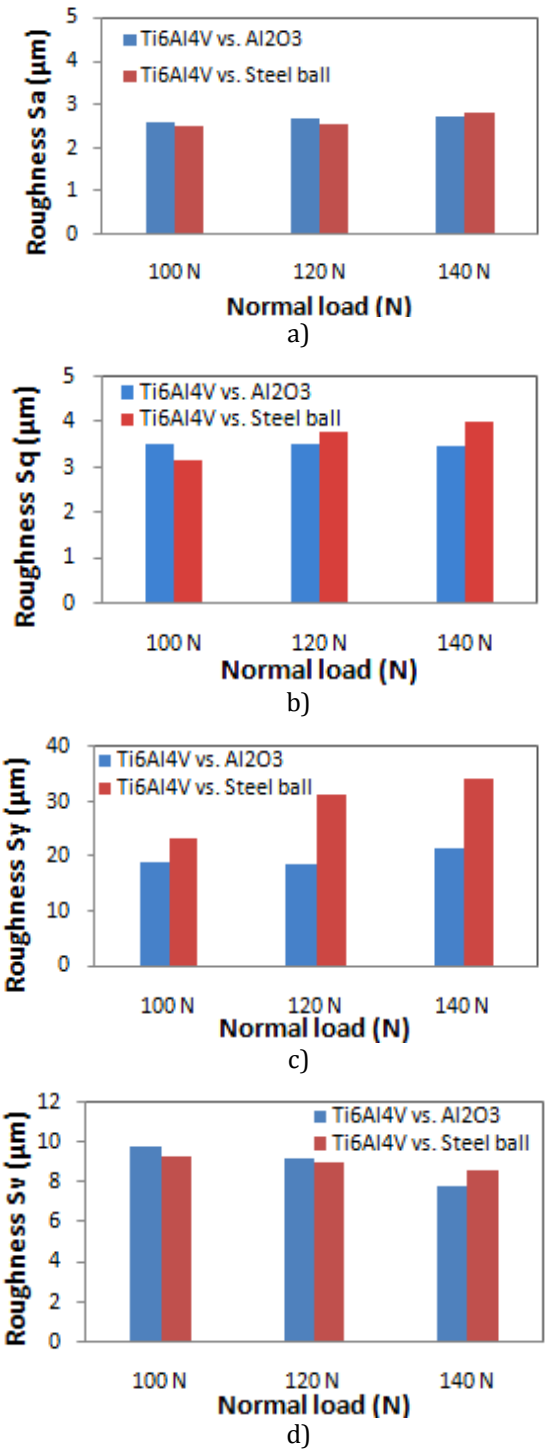

Fig. 6. Evolution of the roughness parameters with increasing applied normal load.

Although the average roughness parameter *Sa* is commonly used in the analysis of the evolution of surface topography, it does not allow to characterize the influence of roughness over the degradation process of a surface or the load level over the evolution of surface topography [17].

The roughness parameter, S_v, (Maximum Valley Depth) is closely related to load level. In this case (Fig. 6d) the constant evolution of this parameter for Ti6Al4V/steel ball contact pair indicates a low affinity of the titanium alloy to the bearing steel.

Similarly can be remarked the affinity of the titanium alloy to ceramic materials (Al_2O_3).

The evolution of the roughness parameter S_q (Root Mean Square) gives indications about the degree of flattening of the profile. It was observed a constant flattening level in the case of Ti6Al4V/Al_2O_3 contact pair. It gives indications about the dimensional stability of this material pairs, and consequently the possibility to use this over a long period.

The evolution of the roughness parameter S_y (Peak-Peak Height) (Fig. 6c) refers to the interdependence between surface roughness and its image. This is based mainly on the functional dependence of roughness height and grey level image of surface, which means that the higher parts of the asperities correspond to higher intensity pixels. Also this parameter indicates the stability of the surface conditions with increasing normal load. This leads to a longer stability of the initial surface conditions during the service life of Ti6Al4V/Al_2O_3 contact pair. The evolution of previous mentioned roughness parameters shows that in terms of surface quality and functional maintenance the Ti6Al4V/Al_2O_3 contact pairs present a higher functional integrity level.

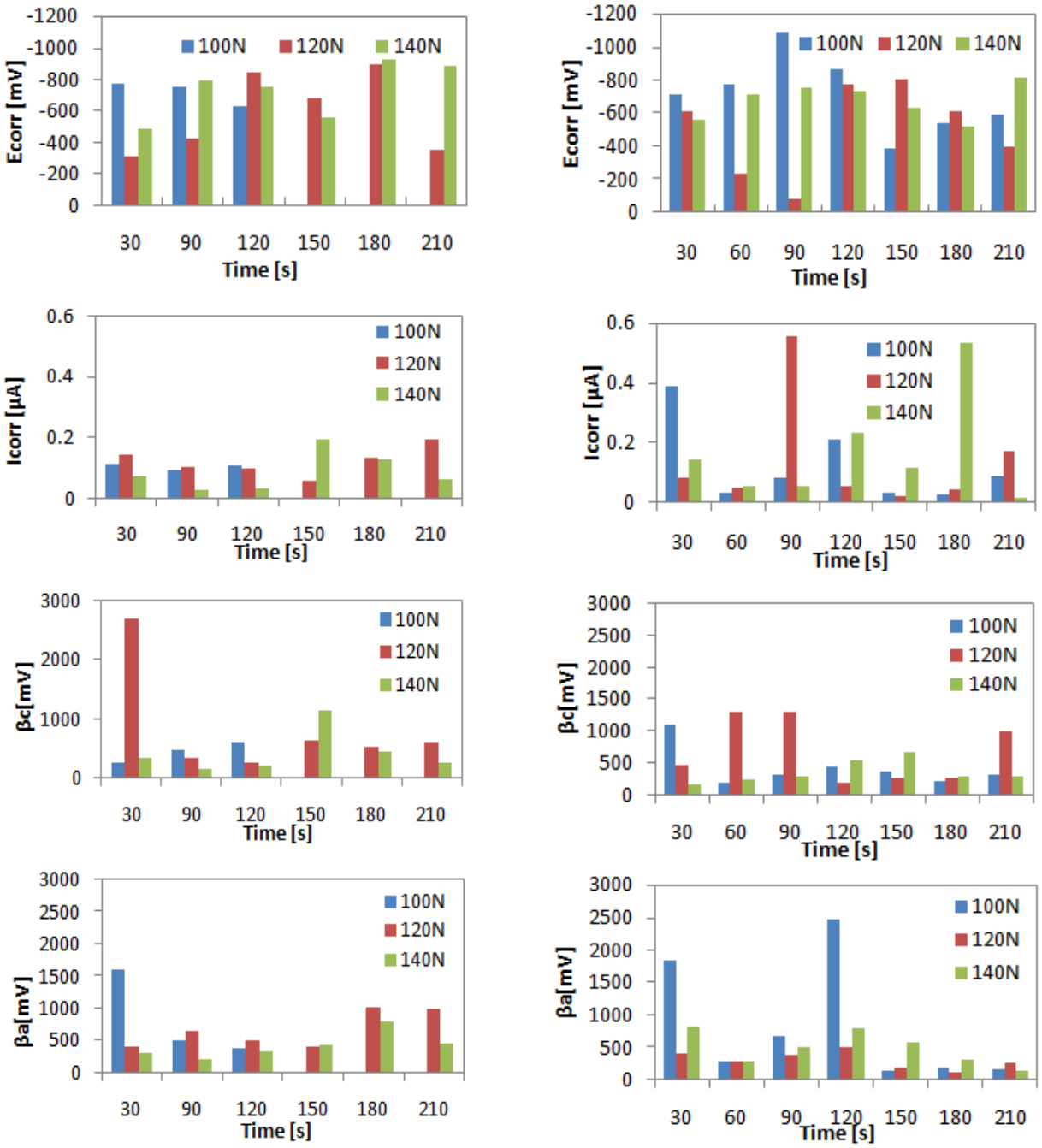

Fig. 7. Evolution of the electrochemical parameters: a) Ti6Al4V/Al_2O_3 and b) Ti6Al4V/steel ball.

Figures 7a and b shows the evolution of the electrochemical parameters for both contact pairs.

The functional integrity of the tests in corrosive environment for both material pairs indicated differences in the evolution of the electrochemical parameters that characterize the electrochemical state of the contact surfaces.

Thus, in the case of Ti6Al4V/Al_2O_3 contact pair (Fig. 7a) at low load levels (100 N) the electrochemical parameters E_{corr} and I_{corr} do not change much with time. Parameters β_a and β_c have significant variation, with an increasing tendency for β_c and a decreasing tendency for β_a. The increase of the applied load changes the evolution of those parameters with time. These will have an oscillatory tendency. In the case of Ti6Al4V/steel ball can be observed a more pronounced oscillatory evolution of all electrochemical parameters with time (figure 7b) at higher load levels than for Ti6Al4V/Al_2O_3 contact pair (except for the evolution of parameter β_c).

The analysis from the functional integrity point of view based on electrochemical criterions

indicates a higher integrity level of Ti6Al4V/Al_2O_3 contact pair.

Figure 8 shows the evolution of coefficient of friction with the sliding distance in the case of dry reciprocating wear tests.

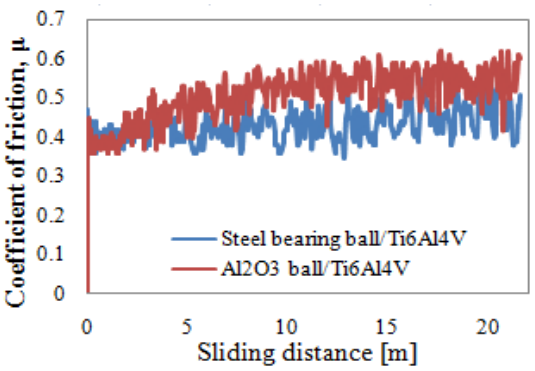

Fig. 8. Evolution of the coefficient of friction with the sliding distance for dry reciprocating wear tests.

Figure 9 shows the evolution of coefficient of friction with the sliding distance in the case of reciprocating wear tests in corrosive environment for both contact pairs.

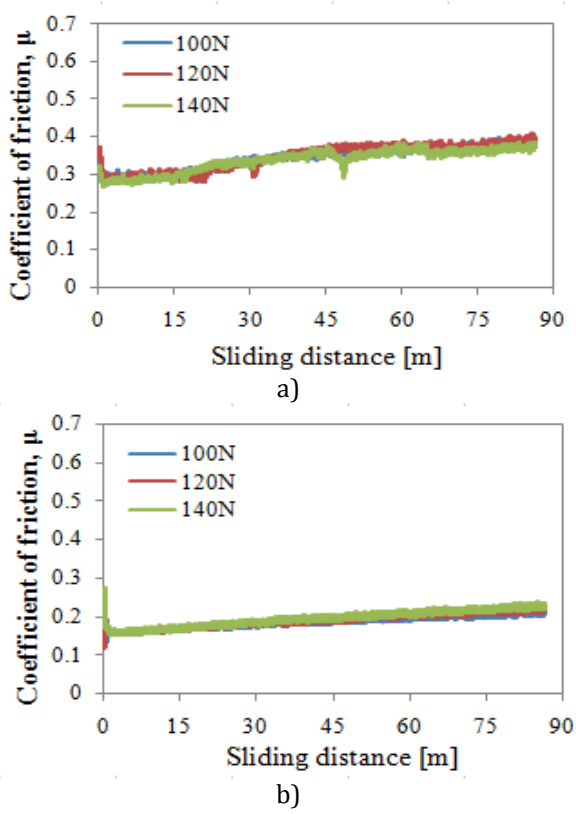

Fig. 9. Evolution of the coefficient of friction with the sliding distance for reciprocating wear tests in corrosive environment: a) /Ti6Al4V/Al2O3 and b) Ti6Al4V/steel ball.

The variation of COF for dry reciprocating wear conditions (Fig. 8) is similar for both contact pairs used in this study. The COF has a slight higher value in the case of Ti6Al4V/Al_2O_3 than Ti6Al4V/steel ball contact pairs.

Also in the case of reciprocating wear in corrosive environment the variation of COF is similar for both contact pairs. The COF was not influenced by the load level. The Ti6Al4V/steel ball (Fig. 9b) contact pair showed a more stable evolution of the COF at a low level than in the case of Ti6Al4V/Al_2O_3 contact pair (Fig. 9a).

5. CONCLUSION

This present paper showed the behavior of a TI6Al4V alloy under reciprocating wear sliding conditions in a comparative way for two different counter materials, bearing steel and ceramic balls (Al_2O_3 - 99.6 %) in dry and corrosive environment (an aqueous solution of 3.5% NaCl). It aimed to highlight the tribological characteristics that shows invariability during the test and provides a high level of functional integrity of the surface.

The conclusions drawn from this work are as follows:

- in dry condition the Ti6Al4V/Al_2O_3 contact pair showed a high functional integrity degree of the surfaces in terms of surface quality, characterized by roughness parameters S_a, S_q and S_y, while for the Ti6Al4V/steel ball based on the roughness parameter S_v;
- in the case of Ti6Al4V/steel ball contact pair a better functional integrity (evaluated based on the weight loss) occurred for higher applied loads than in the case of lower loads;
- from the point of view of the electrochemical behavior a higher functional integrity occurs in the case of Ti6Al4V/Al_2O_3 contact pair at lower applied loads (assessed through parameters E_{corr} and I_{corr});
- the electrochemical parameters for Ti6Al4V/Al_2O_3 contact pair are at a lower level than those of the Ti6Al4V/steel ball contact pair;
- the evolution of the roughness parameters and the structural affinity between TI6Al4V alloy and the bearing ball conduced to a higher functional integrity level from the point of view of the evolution of COF by comparison to Ti6Al4V/Al_2O_3 contact pair.

REFERENCES

[1] B. Griffiths: *Manufacturing Surface Technology-Surface Integrity and Functional Performance*, Prenton Press, 2001.

[2] G. Bellows, D.N. Tisher: *Introduction to surface Integrity Report TM70-974*, Cincinnati: General Electric Co., 1970.

[3] N. Aris, K. Cheng: *Characterization of the surface functionality on precision machined engineering surfaces*, International Journal of Advanced Manufacturing, Vol. 38, No. 3-4, pp. 402-409, 2008.

[4] I.S. Jawahir, E. Brinksmeier, R. M'Saoubi, D.K. Aspinwall, J.C. Outeiro, D. Meyer, D. Umbrello, A.D. Jayal: *Surface integrity in material removal processes: Recent advances*, CIRP Annals - Manufacturing Technology, Vol. 60, No. 2, pp. 603–626, 2011.

[5] L. Deleanu, A. Cantaragiu, I. G. Bîrsan, G. Podaruc. Georgescu: *Evaluation of the Spread Range of 3D Parameters for Coated Surfaces*, Tribology in Industry, Vol. 33, No. 2, pp. 72-78, 2011.

[6] F. Živić, M. Babić, S. Mitrović, P. Todorović: *Interpretation of the Friction Coefficient During Reciprocating Sliding of Ti6Al4V Alloy Against Al2O3*, Tribology in Industry, Vol. 33, No. 1, pp. 36-42, 2011.

[7] F. Živić, M. Babić, N. Grujović, S. Mitrović: *Tribometry of Materials for Bioengineering Applications, Tribology in Industry*, Vol. 32, No. 1, pp. 25-32, 2010.

[8] J.F. Archard: *Wear theory and mechanisms*. In: M.B. Peterson, W.O. Winer, Wear Control Handbook. ASME, 1980.

[9] R.J.K. Wood: *Tribo-corrosion of coatings: a review*, J. Phys. D: Appl. Phys., Vol. 40, No. 18, pp. 5502–5521, 2007.

[10] P. Ponthiaux, F. Wenger, D. Drees, J.P. Celis: *Electrochemical techniques for studying tribocorrosion processes*, Wear, Vol. 256, No. 5, pp. 459–468, 2004.

[11] S. Mischler, S. Debaud, D. Landolt: *Wear-accelerated corrosion of passive metals in tribocorrosion systems,* Journal of the Electrochemical Society, Vol. 145, No. 3, pp. 750-758, 1998.

[12] J. Perret: *Modélisation de la tribocorrosion d'aciers inoxydables dans l'eau à haute pression et haute température*, Thèse No 4727 École Polytechnique Fédérale De Lausanne, 2010.

[13] S. Feliu, J.A. Gonzalez, S. Miranda: *Possibilities and Problems of in Situ Techniques for Measuring Steel Corrosion Rates in Large Reinforced Concrete Structures,* Corrosion Science, Vol. 47, No. 1, pp. 217-238, 2005.

[14] H.H. Uhlig, R.W. Revie: *Corrosion and Corrosion Control*, 3rd Edition, John Wiley and Sons, New York, 1985.

[15] B. Bobic, S. Mitrovic, M. Babic, A. Vencl, I. Bobic: *Corrosion Behavior of the As-cast and Heat-treated ZA27 Alloy*, Tribology in Industry, Vol. 33, No. 2, pp. 87-93, 2011.

[16] M. Stern, A.L. Geary: *Electrochemical Polarization, A Theoretical Analysis of the Shape of Polarization Curves*, Journal of Electrochemical Science, Vol. 104, No. 1, pp. 56-63, 1957.

[17] V. Mereuta, M. Buciumeanu, L. Palaghian: *3D Roughness Parameters as Factors in Determining the Evolution of Effective Stress Concentration Factors in Fatigue Processes*, Applied Mechanics and Materials, Vol. 248, pp. 504-510, 2013.